Optica Applicata, Vol. IX, No. 1, 1979

Detection of thermal radiation by 77–300 K (CdHg)Te detectors

JÓZEF PIOTROWSKI, TADEUSZ PIOTROWSKI

Military Academy of Technology, Warsaw, Poland.

The normalized thermal figure of merit M^* of (CdHg)Te photoconductive detectors has been calculated. It has been assumed that Auger recombination is the main mechanisms limiting the lifetime of this material. The dependences of the M^* value on detector cut-off wavelength, detector temperature (in the range of 77–300 K) and object temperature (in the range of 100–1000 K) have been evaluated. The obtained experimental data of M^* have been used to compare (CdHg)Te detectors with thermal detectors (pyroelectric detectors and thermocouples). It has been stated that in low frequency range ($f < 100$ Hz) thermal detectors are better for detection of room temperature objects than noncooled (CdHg)Te detectors, while for higher frequencies (CdHg)Te detectors are better. The same is true also for the photon (CdHg)Te detectors cooled down to 250 K. The advantage of photon detectors over thermal detectors increases with the object temperature.

Introduction

The basic parameters of the detectors for thermal radiation are thermal voltage responsivity R_{VT} and normalized thermal figure of merit M^*. The concepts of these parameters have been introduced in [1] and defined as:

$$R_{VT}(T_0) = \int_0^\infty R_V(\lambda) \frac{\partial m(\lambda, T_0)}{\partial T} d\lambda, \tag{1}$$

$$M^*(T_0) = \int_0^\infty D^*(\lambda) \frac{\partial m(\lambda, T_0)}{\lambda T} d\lambda, \tag{2}$$

where:

$m(\lambda, T) = C_1 \lambda^{-5} \left(\exp \frac{C_2}{\lambda T_0} - 1\right)^{-1}$ – Planck's distribution,

$C_1 = 2\pi hc^2 = 3.74 \times 10^{-16}$ W m^2,

$C_2 = hc/k = 1.44 \times 10^{-2}$ K m,

T_0 – object temperature.

Thermal responsivity (1) enables to evaluate the signal voltage obtained from detectors exposed to the thermal radiation of the object. Normalized thermal figure of merit M^* (2) describes detectability for the thermal radiation and is used for evaluation of noise equivalent temperature difference (NETD). Thermal figure of merit allows to evaluate univocally the usefulness for the detection of the objects radiation and to compare the detectors with different spectral characteristics.

Evaluation of the limits of photoconductive (CdHg)Te detector parameters

The values of thermal responsivity and normalized thermal figure of merit can be obtained by means of numerical integration of measured or theoretically calculated spectral response of the detector. They can be also determined experimentally.

When estimating the quality of photon detectors the spectral response is identified in practice with that of ideal photon counter:

$$D^*(\lambda) = \begin{cases} \dfrac{\lambda}{\lambda_{co}} D^*(\lambda_{co}) & \text{for} \quad 0 < \lambda \leqslant \lambda_{co}, \\ 0 & \text{for} \quad \lambda > \lambda_{co}. \end{cases} \tag{3}$$

Taking also $\lambda_p = \lambda_{co}$,

where:

λ_p — peak wavelength,

λ_{co} — cut-off wavelength,

we obtain

$$R_{VT}(T_0) = R_V(\lambda_{co}) \int_0^{\lambda_{co}} \frac{\lambda}{\lambda_{co}} \frac{\partial m(\lambda, T_0)}{\partial T} d\lambda, \tag{4}$$

$$M^*(T_0) = D^*(\lambda_{co}) \int_0^{\lambda_{co}} \frac{\lambda}{\lambda_{co}} \frac{\partial m(\lambda, T_0)}{\partial T} d\lambda. \tag{5}$$

The above relations are used for evaluation of thermal responsivity and figure of merit M^*.

The integrals depend only on cut-off wavelength and object temperature and can be calculated by numerical integration. In case of (CdHg)Te photoconductive detectors the dependence of the limit D^* on λ_{co} [2] is

$$D^* = 0.64 \frac{\lambda_{co}}{hc} \left(\frac{\alpha \tau_i}{n_i} \right)^{1/2}, \tag{6}$$

where:

α — absorption coefficient,

τ_i — intrinsic recombination time,

n_i — intrinsic carrier concentration,

h — Planck constant,

c — velocity of light.

This expression gives the optimal value of normalized detectivity for photoconductive detector made of intrinsic material when Auger recombination prevails ($\tau_i = \tau_{A_i}$).

For these detectors the dependence of figure of merit M^* on cut-off wavelength, object temperature (T_0) and detector temperature (T) are shown in fig. 1. Some experimental data are also presented.

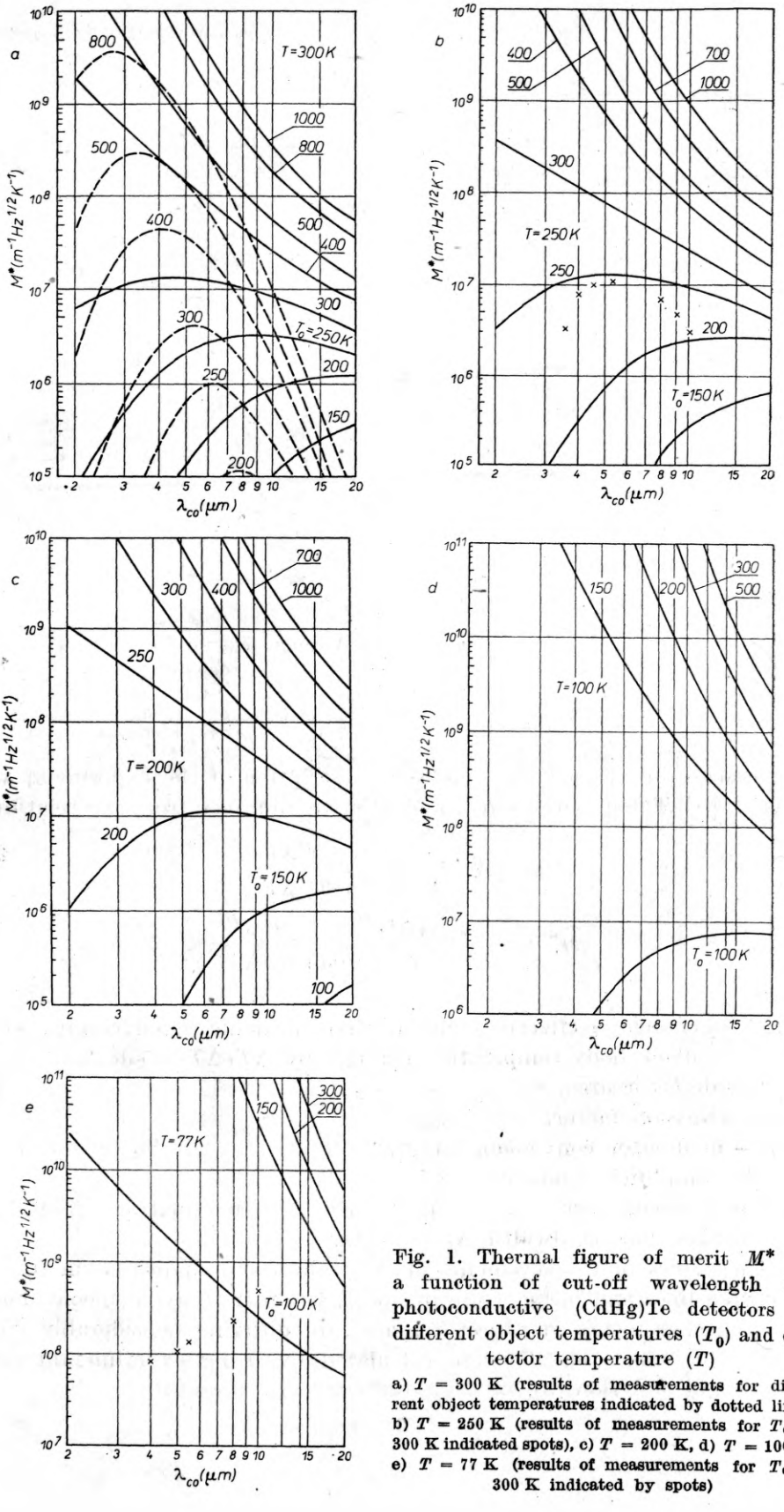

Fig. 1. Thermal figure of merit M^* as a function of cut-off wavelength for photoconductive (CdHg)Te detectors at different object temperatures (T_0) and detector temperature (T)

a) T = 300 K (results of measurements for different object temperatures indicated by dotted line), b) T = 250 K (results of measurements for T_0 = 300 K indicated spots), c) T = 200 K, d) T = 100K, e) T = 77 K (results of measurements for T_0 = 300 K indicated by spots)

Experimental

Block diagram of the arrangement for R_{VT} and M^* measurements is presented in fig. 2. This arrangement was designed mainly for near room

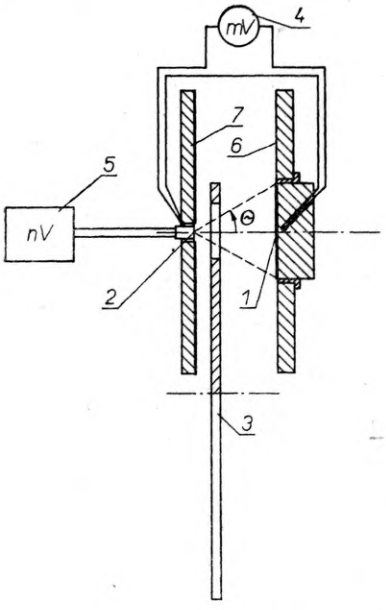

Fig. 2. Arrangement for R_{VT} and M^* measurements:
1 – black body, *2* – detector, *3* – modulator, *4* – temperature indicator, *5* – amplifier and readout, *6* – low emissivity shield, *7* – high emissivity shield

temperature investigations. A detailed description of the experiment was given in [3]. The quantities R_{VT} and M^* were obtained from the relations:

$$R_{VT} = \frac{1}{A \cdot \varepsilon \cdot \varkappa \sin^2 \theta} \frac{\Delta V}{\Delta T}, \tag{7}$$

$$M^* = \frac{(\Delta f)^{1/2}}{(\overline{U}_n^2)^{1/2} A^{1/2} \varepsilon \cdot \varkappa \cdot \sin^2 \theta} \frac{\Delta V}{\Delta T}, \tag{8}$$

where:

ΔV – change of effective value of first harmonic signal voltage when black body temperature changes by $\Delta T (\Delta T \leqslant 5$ deg),

A – detector area,

ε – emission factor,

$\varkappa$ – modulator conversion factor,

Δf – amplifier bandwidth.

The measurements were performed at modulation frequency $f = 1000$ Hz and bandwidth $\Delta f = 18$ Hz.

The results of measurements of M^* values area indicated in fig. 1a by dotted lines and in fig. 1b, e by spots. In order to avoid inconvenient direct measurements at object temperature differing considerably from 300 K, the values of M^* were calculated by using experimental data $D^*(\lambda_{co})$ and equation (5).

Discussion

The dependences given in fig. 1 refer to detectors both noncooled and cooled by the following commonly used methods:

- thermoelectric one-step cooling ($T_d = 250$ K),
- thermoelectric two- and more-step cooling ($T_d = 200$ K–100 K),
- liquid nitrogen cooling ($T_d = 77$ K).

With decreasing detector temperature rapid increase of maximum M^* value is observed for both theoretical and experimental values. Theoretical M^* values result from the assumed detector performance model and carrier recombination mechanism. They determine upper limit of M^*. The plots $M^*(\lambda_{co})$ show a sharp maximum for the given $\lambda_{co\,max}$ (fig. 1a), which is sharper for experimental than for theoretical curves. This maximum shifts towards short wavelength with the increasing temperature of object, since the optimum value of λ_{co} depends on the latter.

From comparison of theoretical and experimental curves $M^*(\lambda_{co})$ for $T = 300$ K it follows that at different object temperatures the optimum λ_{co} values are more divergent for theoretical than for experimental data. When the object and detector temperatures are equal these maxima coincide. When the object temperature is lower than that of detector the shift of theoretical maximum towards long wavelengths is more rapid than that of the experimental one. For $T_0 > T$ this shift occurs in the opposite direction.

From the above dependences it may be concluded that for the measurements of thermal radiation from objects of near 300 K temperature the best noncooled photoconductive detector is that with cut-off wavelength λ_{co} of about 5.5 μm. This is an edge of atmospheric window 3–5.5 μm. For such detectors the maximum value of M^* is 4×10^6 m^{-1} Hz$^{1/2}$ K^{-1} which is about three times lower than the theoretical limiting value and about 25 times lower than the value given by background noise for BLIP detector [4].

It should be noticed that at modulation frequency $f = 100$ Hz the best experimental M^* are the same and that they decrease considerably with the increasing frequency.

Some experimental M^* values for cooled detectors are marked in fig. 1b, e. Detectors cooling causes that the experimental values of M^* rise much slower than the theoretical ones. Consequently, the difference between theoretical and experimental curves increases with the cooling deepness. Moreover, at all modulation frequencies experimental values of M^* for cooled (CdHg)Te detectors are much higher than for thermal detectors.

In deeply cooled (CdHg)Te detectors there appears an additional M^* limitation caused by background radiation [4].

Summarizing remarks

Limiting values of M^* for photoconductive (CdHg)Te detectors have been evaluated and verified experimentally. Numerical dependences $M^*(\lambda_{co})$ for different object and detector temperatures have been given. Differences between experimental and theoretical curves $M^*(\lambda_{co})$ are simply due to the differences between experimental and theoretical D^* values.

For the measurements of thermal radiation of near 300 K temperature objects the best uncooled photoconductive detector is that of wavelength cut-off $\lambda_{co} = 5.5$ μm. Its M^* value is close to detectivity of thermal detector working at modulation frequency $f = 100$ Hz and considerably exceeds the latter when modulation frequency is higher than 1 kHz [5]. This advantage becomes more pronounced with rising object and falling temperature of the detector.

The above mentioned detectors have been applied to photoelectric pyrometers for object temperatures of 300–800 K [6] and to experimental thermal imaging devices.

The dependences of M^* values limit on wavelength cut-off, object and detector temperatures as well as its experimental data may be used to estimate the usefulness of detectors in devices designed for temperature measurements and for thermal imaging systems.

References

[1] CHIARI J. A., JERVIS M. H., Proc. Inter. Conf. Electro-Optics, Brighton 1971
[2] PIOTROWSKI J., PIOTROWSKI T., Biuletyn WAT **27**, 131 (1978).
[3] GALUS W., KILIAS J., PIOTROWSKI J., PIOTROWSKI T., Biuletyn WAT **26**; 137 (1977).
[4] LONGSHORE R., RAIMONDI P., LUMPKIN M., Infrared Phys. **16**, 639 (1976).
[5] MORTEN F. D., Proc. of Low Light Level and Thermal Imaging System Conference, London 1975.
[6] KILIAS J., NOWAK Z., PIOTROWSKI J., PIOTROWSKI T., Pomiary, Automatyka, Kontrola **23**, 441 (1977).

Received, December 17, 1977

Детектирование теплового излучения с помощью детекторов (CdHg)Te температурами (77-300K)

Произведен расчет тепловой обнаруживаемости стандартной M^* для фотопроводящих детекторов (Cd, Hg)Te при предположении, что долговечность в самостоятельном материале определена рекомбинацией Оже. Приведены графики зависимости M^* от порога длинноволнового детектора и от температуры объекта (в интервале 100–1000 К) для нескольких значений температур детекторов (в интервале 77–300 К). С использованием полученных значений M^* сравнены детекторы (Cd, Hg)Te с тепловыми детекторами.

Обнаружено, что при детектировании излучения объектов температурой 300 К не охлаждаемые детекторы (Cd, Hg)Te уступают тепловым детекторам (пироэлектрическим и тер-

мопарам) только в области низких частот модуляции ($f \leqslant 100$ Гц); они оказываются лучше термических при более высоких частотах. При более высоких температурах объекта обнаруживается заметное превосходство фотонных детекторов. Фотонные детекторы (Cd, Hg)Te, охлаждаемые до температуры 250 К и ниже, превосходят тепловые детекторы и в пределах низких частот.